

Heterogeneous nature of relaxation dynamics of Room Temperature Ionic Liquids (EMIm)₂[Co(NCS)₄] and (BMIm)₂[Co(NCS)₄]

Stella Hensel-Bielowka¹, Zaneta Wojnarowska², Marzena Dzida¹, Edward Zorębski¹, Michał Zorębski¹, Monika Gęppert-Rybczyńska¹, Tim Peppel³, Katarzyna Grzybowska², Yangyang Wang⁴, Alexei Sokolov^{5,6}, Marian Paluch²

¹*Institute of Chemistry, University of Silesia, Szkolna 9, 40-006 Katowice, Poland*

²*Institute of Physics, University of Silesia, Uniwersytecka 4, 40-007 Katowice, Poland*

SMCEBI, University of Silesia, 75 Pulku Piechoty, 41-500 Chorzow, Poland

³*Leibniz Institute for Catalysis, Albert-Einstein-Str. 29a, 18059 Rostock, Germany,*

⁴*Center for Nanophase Materials Sciences, Oak Ridge National Laboratory, Oak Ridge, Tennessee, 37831, USA*

⁵*Chemical Sciences Division, Oak Ridge National Laboratory, Oak Ridge, Tennessee 37831, USA*

⁶*Department of Chemistry, University of Tennessee Knoxville, Knoxville, Tennessee 37996, USA*

Abstract

Dynamic crossover above T_g has been recognized as a characteristic feature of molecular dynamics of liquids approaching glass transition. Experimentally it is manifested for example as a change in Vogel-Fulcher-Tamman dependence or a breakdown of the Stokes-Einstein and related relations. In this letter we report the exception from this rather general pattern of behavior. By means of dielectric, ultrasonic, rheological and calorimetric methods dynamics of ionic liquids (BMIm)₂[Co(NCS)₄] and (EMIm)₂[Co(NCS)₄] was studied in a very broad temperature range. However, none of the mentioned dynamic changes was observed in the entire studied temperature range. On the contrary, the single VFT and the same fractional Walden coefficient were found for a conductivity and viscosity changes over 12 decades. Moreover, ultrasonic studies revealed that the data at temperatures which cover the normal liquid region cannot be fitted by a single exponential decay, and Cole-Cole function should be used instead.

Ionic liquids (ILs) have triggered great interest in both scientific and industrial society. Their special attraction lies in their unique properties like huge range of fluidity, chemical and thermal stability, high conductivity ($>10^{-4}\text{S}^*\text{cm}^{-1}$) or large electrochemical window together with fast ion mobility that makes them especially promising candidates for electrochemical applications¹. Furthermore, many of them are non-volatile and non-flammable, although nowadays it is obvious that these properties are not general². Also their impact on natural environment is not as neutral as it was thought earlier, although they are still regarded as “green” chemicals. Another branch of industry interested in special properties of ILs is pharmacy.^{3,4} Among different classes of ILs metal-containing ones attract particular attention of researchers due to properties that cannot be associated with typical ILs⁵. Unfortunately, the most popular ILs with halogenometalate complexes as anions turn out to be unstable⁵. A new class of substances are liquids with thio- and isothiocyanatometalates of transition metals in anions⁶. In the previous papers^{7,8} few basic properties of newly synthesized paramagnetic 1-alkyl-3-methylimidazolium ionic liquids $(\text{EMIm})_2[\text{Co}(\text{NCS})_4]$ and $(\text{BMIm})_2[\text{Co}(\text{NCS})_4]$ were reported. These substances appeared to have many features interesting for engineers^{7,8}. However, their chemical structure and less common stoichiometry makes them also very interesting from the point of view of basic science. Recently molecular dynamics of supercooled and glassy ILs have been extensively studied. An in-depth knowledge of molecular dynamics’ behavior near T_g of ionic liquids is also necessary to formulate complete theory of a liquid-glass transition. Thus, we decided to expand the scope of our interests beyond the common physicochemical characteristic of these materials. In this paper, we focused on the molecular dynamics of both mentioned ILs in normal and supercooled liquid as well as in a glassy state. Combining ultrasonic, dielectric, rheological and calorimetric methods we were able to trace evolution of dynamical properties of studied samples over 12 decades, down to the glass transition temperature. Details of each experiment can be

found in the supplementary materials. As a result we observed several interesting phenomena like non-Newtonian behavior, lack of the dynamical crossover in the range of 1.2-1.5T_g and slight decoupling between conductivity and structural relaxation times. Since (EMIm)₂[Co(NCS)₄] and (BMIm)₂[Co(NCS)₄] behave differently than commonly noted for ionic liquids, it provides better understanding the mechanisms governing molecular dynamics of such type of substances over a very wide temperature range, including the supercooled state.

Generally speaking, the ionic liquids (EMIm)₂[Co(NCS)₄] (**I**) and (BMIm)₂[Co(NCS)₄] (**II**) are relatively easy to supercool. However, the first one shows some tendency to crystallization that is in agreement with other imidazole-based ILs.⁵ In this case a cold crystallization was observed at $T_c = 264\text{K}$ with melting point at $T_m = 292\text{K}$ when heated with a rate of 5K/min. The crystallization process does not occur at higher heating rates.

Dielectric spectra were measured in a temperature range from below T_g (208K for (**I**) and 209 for (**II**)) up to 293.15K for (BMIm)₂[Co(NCS)₄] and 233.15K for (EMIm)₂[Co(NCS)₄]. Usually the dielectric data of conducting materials are analyzed in either conductivity or electrical modulus representation. Both representations trace the same phenomena and are interrelated with each other. The results in both representations are shown in Fig 1a, b and Fig 1c, d for (**I**) and (**II**) respectively. In an imaginary part of modulus spectra (M'') the dominant feature is the asymmetric peak of the σ -relaxation. The inverse of the frequency of M'' peak maximum designates the relaxation time ($\tau_\sigma = 1/2\pi f_{max}$).

Values of the dc-conductivity at a given temperature can be determined from the plateau region in the middle part of the conductivity spectrum. The temperature dependence of the dc-conductivity, presented in Figure 2, is very similar for both samples although, as expected, values of conductivity of (EMIm)₂[Co(NCS)₄] are a bit higher due to the fact that shorter side chain makes these cations more mobile. For (BMIm)₂[Co(NCS)₄] we were able to carry out dielectric

measurements in a wider temperature range due to the lack of tendency to crystallization. Analysis of conductivity data obtained for sample (II) reveals unexpected behavior with decreasing temperature. In many fragile liquids (liquids with strongly non-Arrhenius temperature variations of relaxation time) the temperature dependence of relaxation times reveals several characteristic changes: At high temperatures it follows an Arrhenius law; then at some T_A it changes to a VFT dependence; and at some T_B between T_A and T_g it usually crosses over to another VFT. This T_B usually appears in the range $\sim 1.2\text{-}1.5T_g^9$. The last change of the temperature dependence of relaxation times is observed at T_g where temperature dependence crosses over to an Arrhenius type. Among different views on the origin of the dynamic crossover at T_B the most common ascribes it a temperature below which cooperativity becomes a crucial factor and where dynamical heterogeneity of the system starts to play a key role in the molecular dynamics^{10,11}. The change of VFT dependence at T_B was observed for small molecular liquids like OTP¹², diisobutyl phthalate¹³ and polymers like polyisoprene¹⁴.

Surprisingly, a close examination of Figure 2 reveals that for sample (II) a single VFT in a form:

$$\sigma = \sigma_\infty \exp\left(\frac{-DT_0}{T - T_0}\right) \quad (1)$$

(with σ_∞ - conductivity at infinite temperature, T_0 – temperature of an ideal glass transition and D - a strength parameter) can perfectly describe the temperature dependence of σ in the entire temperature range above T_g . To make our experimental range of temperatures even broader we added to Figure 2 conductivity data obtained by Geppert-Rybczyńska^{7,8} in a normal liquid state at temperatures as high as 333K which is around $1.6T_g$.

The best way to identify precisely the existence of any specific changes in temperature dependence of the interested transport coefficient is to analyze the experimental data by means of

the so-called Stickel's derivative operators¹⁵. These operators linearize VFT (eq.1) and transform Arrhenius relation

$$\sigma = \sigma_\infty \exp\left(\frac{-E_a}{RT}\right) \quad (2)$$

into a constant value according to the following equation (in the case of Arrhenius relation $T_0=0$):

$$[d \log(x)/d(1/T)]^{-1/2} = (B)^{-1/2} * (1 - T_0/T) \quad (3)$$

where x is the studied property, B - a respective constant. Thus, any change in the temperature dependence of x should be visible as an intersection of straight lines. The result of such analysis for $(\text{BMIm})_2[\text{Co}(\text{NCS})_4]$ is presented in the inset in Figure 2. It clearly shows that the only visible crossover occurs around 209K and is related to crossing the glass transition. On the other hand no clear indication of existence of T_B exists up to $1.6T_g$. Similar picture can be obtained for viscosity. Result of Stickel's analysis for viscosity data of **(II)** is shown in upper right inset to Figure 2. Again when we add the data from ref. 17, no signs of the dynamical crossover can be found at any temperature up to 323K $\sim 1.5T_g$. It is worth mentioning that the same pattern of behavior was previously found also for $(\text{BMIm})[\text{PF}_6]$, $(\text{BMIm})[\text{NTf}_2]$ and $(\text{BMIm})[\text{TFA}]^{16}$ for which temperature dependence of structural relaxation times and diffusion coefficient were studied. The question arises immediately whether it can be more general behavior of ILs. In this context, it has to be noted that all the ILs studied by Griffin¹⁶ contained BMIm cation similarly to our sample. It is interesting that one of the very few known molecular liquids for which T_B is not observed is di-n-butyl phthalate. It turns out that structure of di-n-butyl phthalate¹³ slightly resembles BMIm cation. Thus, also their behavior may be similar.

Temperature dependence of σ -relaxation times are presented in Figure 3a and b for **(I)** and **(II)** respectively. It is commonly believed that for ILs, temperature dependence of σ and τ_σ

follows that of shear viscosity η , as expected from the Walden rule for conductivity in molecular liquids. However, it was shown for several ionic materials that there is a decoupling between viscosity (structural relaxation) and conductivity (conductivity relaxation). It is especially prominent for protic ionic liquids¹⁷ due to enhanced proton conduction caused by Grotthuss mechanism.

In Figure 3 glass transition is demonstrated as a crossover from VFT (eq.1) to Arrhenius (eq.2) temperature dependence of σ -relaxation times. We compared these data with the viscosity and specific heat relaxation, which reflect the structural relaxation. It is clearly visible in Figure 3 that a slight decoupling between studied properties takes place, in violation of the classical Walden rule. Instead fractional Walden rule $\Lambda_0 \eta^b = \text{const}$ can be used, where b is a measure of decoupling. In our case b values equals 0.91 and 0.95 for samples (I) and (II) respectively (see the inset in Figure 3). The decoupling of diffusion and structural relaxation (viscosity) has been found in many glass forming liquids, but usually only for temperatures below T_B ¹⁸. For our samples almost the same values of the exponent b were obtained in the entire temperature range. This observation strengthens our view that no change in the dynamics occurs in the range of 1.2- $1.5T_g$.

Further interesting details can be revealed from studies of the ultrasound absorption in normal liquid range. The ultrasound absorption coefficient α per squared frequency f , *i.e.* the product $\alpha \cdot f^2$ for both liquids are summarized in Table 3 of supplementary materials. As evidenced from this table and Figures 4a and 4b, the dependence of the quotient αf^{-2} on frequency changes strongly with temperature. It appears also that within the investigated frequency range the quotient αf^{-2} is clearly dependent on frequency as high as above 10 MHz. Thus, in both cases the dispersion characteristics $d(\alpha f^{-2})/df < 0$ is observed. Moreover, both liquids are rather highly absorbing,

i.e., the frequency normalized attenuation (at $T = 298.15$ K and $f = 100$ MHz) are $837 \cdot 10^{-15}$ and $1321 \cdot 10^{-15}$ $\text{s}^2 \cdot \text{m}^{-1}$, respectively. At the same time it is observed in both liquids that above some frequency, the experimental values of αf^{-2} are smaller than those predicted by the Navier-Stokes relation (α_{cl}). In other words, the absorption curves shown in Figure 4 indicate that $\alpha > \alpha_{\text{cl}}$ at lower frequencies and $\alpha < \alpha_{\text{cl}}$ at higher frequencies, and that the frequency for which $\alpha = \alpha_{\text{cl}}$ decreases with the increasing temperature. Most probably this kind of behavior results from a relaxation mechanism of the viscous type. Similar behavior has been reported previously for several molecular liquids 1-dodecanol¹⁹ and castor oil²⁰, diols²¹ as well as ionic liquids (OMIm)NTf₂²² and a series of C_n MIm [PF₆]²³.

The obtained numerical values of $\alpha_{\text{cl}} f^{-2}$ are summarized in Table 4 of the supplementary material. Shear viscosity used for calculations were taken from [7,8].

The small ratio of the observed absorption to that calculated from the Stokes rule (*i.e.*, classical absorption) and the negative temperature coefficients of the experimental absorption in the non-dispersive region are observed for both liquids. These findings are characteristic for liquids with structural relaxation, *i.e.*, for liquids from group III according to liquid classification in relation to absorption data²⁴. Detailed inspection of Table 4 shows that for (I), $\alpha/\alpha_{\text{cl}}$ is temperature independent. This finding indicates an equal temperature dependence of the volume viscosity, η_V , and shear viscosity. On the other hand, for (II) this ratio decreases with temperature. Similar scenario was observed in the case of (EMIm) and (OMIm)NTf₂²². It means that changes in the alkyl chain cause the detectable differences in molecular mechanisms of the volume and shear viscosity. However, in the case of (OMIm) cation the temperature dependence was weaker in comparison to that observed for (II). Immediately the question arises, whether it is anion dependent. Another possible scenario is that there is a maximum of difference for cations

with alkyl substituent between C₂ and C₈ beyond which again the molecular mechanisms of the volume and shear viscosity become similar.

From the frequency dependent ultrasonic absorption data, relaxation times can be obtained via the relation:

$$\alpha \cdot f^{-2} = \sum_{i=1}^n A_i \cdot (1 + (f / f_{i,rel})^2)^{-1} + B \quad (5)$$

where A_i and $f_{i,rel}$ are the relaxation amplitudes and relaxation frequencies, respectively. B represents the sum of the classical part of absorption and contributions from processes with relaxation frequencies considerably higher than $f_{i,rel}$. It appears that for the studied liquids, the frequency dependence of ultrasonic absorption data cannot be fitted with a single Debye-type relaxation processes (n=1). It is in odd to what is commonly observed for ultrasonic spectra of both molecular and ionic liquids in a normal liquid regime^{21,22}. Thus, in this paper we would like to discuss fitting with a stretched function (shape parameters (α and β) should be introduced to the equation (5)). We found that not a Cole-Davidson but a symmetrical Cole-Cole function with the shape parameter (α_{CC}) around 0.8 provides the best fit (full results are given in a Table 5 of a supplementary materials). The relaxation times denoted as τ_{sound} (calculated as $\tau_{rel} = (2 \cdot \pi \cdot f_{rel})^{-1}$) can be found in Figure 3. The symmetrical shape of the spectra is puzzling. A possible explanation is that the process which can be observed by ultrasonic method does not reveal features of the α relaxation but of the β -one. In fact, it was reported several times that in shear mechanical spectra amplitude of the β -process at low temperatures far exceeds the one observed for dielectric spectra. Moreover, it increases much faster with temperature²⁵. Thus, it is very likely that for such high frequencies as used in the ultrasonic method it is the dominant relaxation

process. In such case our samples would be examples of scenario I according to Donth and co-workers²⁶.

With the elongation of the alkyl chain the influence of the non-polar domains increases and C2 atom involved in H-bonds with sulphur atom of the anion²⁷ becomes less acidic. This probably causes higher decoupling in sample (**I**) and differences in ultrasound absorption. On the other hand it is not fully understood whether sterical hindrance, various types of interactions (Coulomb interactions, H-bonds) between cations and anions or non-Newtonian nature of studied liquids are the reasons why the dynamical crossover with all accompanying phenomena is not observed in the region of 1.2-1.5T_g. In fact, it remains an open question whether the observations (lack of change in VFT dependence at T_B, lack of the point in which Walden rule breaks down and symmetrically stretched ultrasonic absorption spectra at high temperatures) are related to each other and whether each of them indeed can be treated as an indicator for existence/nonexistence of a dynamical crossover. However, all our experimental data seem to indicate that the dynamical heterogeneity and cooperativity play a role in the molecular dynamics of ionic liquids studied herein not only in the vicinity of T_g, but also in normal liquid state at least up to 1.6T_g. It means that even at temperatures much higher than T_g they behave like supercooled not like normal liquids. More experimental data in broad temperature range are necessary to answer the question whether it is a general rule for ILs or it is only specific feature of samples based on BMIm cation.

Acknowledgments The authors SHB, ZW, KG, MP are grateful for the financial support by the National Science Centre within the framework of the Opus project (grant no. DEC-2011/03/B/ST3/02072). AS and YW acknowledges financial support from NSF under the grant CHE-1213444.

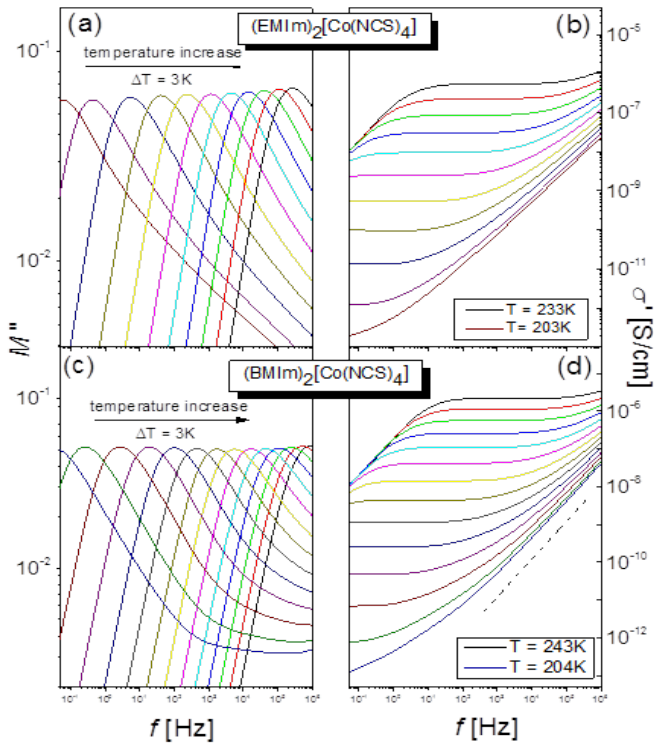


Figure 1

Representative spectra of imaginary part of modulus and real part of conductivity for $(\text{EMIm})_2[\text{Co}(\text{NCS})_4]$ (a,b) and $(\text{BMIm})_2[\text{Co}(\text{NCS})_4]$ (c,d). Dashed line in panel (d) shows the slope equal to 1. The horizontal arrow indicates the direction of the experiment

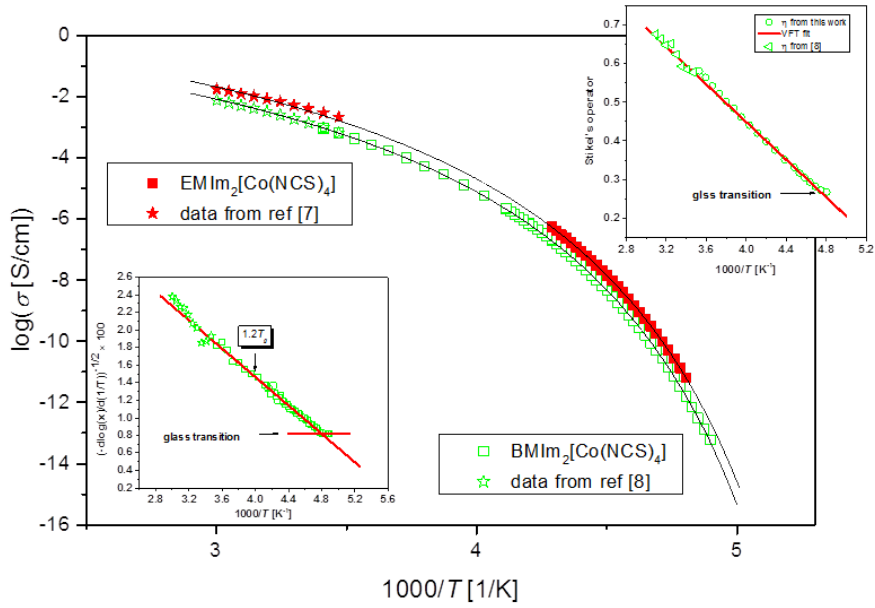


Figure 2

Activation plot of the conductivity of $(EMIm)_2[Co(NCS)_4]$ (solid squares) and $(BMIm)_2[Co(NCS)_4]$ (open squares). (ψ) and (ξ) data from references 7 and 8 respectively. Solid lines are fits by means of eq.1 (parameters are given in Table 1 of supplementary materials). Left lower inset: Stickel's analysis for conductivity data of $(BMIm)_2[Co(NCS)_4]$. Right upper inset: Stickel's analysis for viscosity data of $(BMIm)_2[Co(NCS)_4]$.

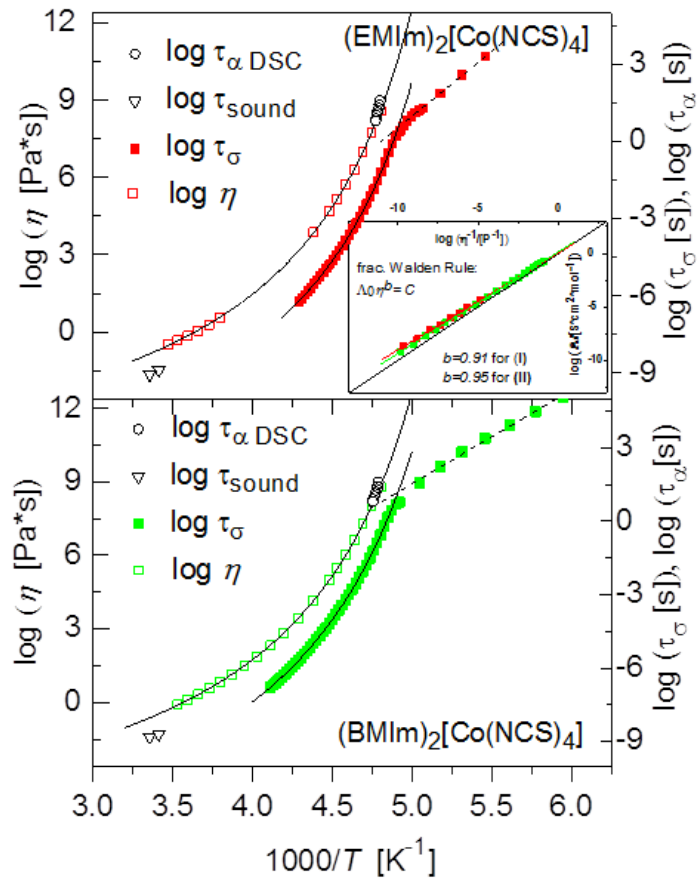


Figure 3

Relaxation map of (a) (EMIm)₂[Co(NCS)₄] and (b) (BMIm)₂[Co(NCS)₄]. Conductivity relaxation times are compared with viscosity and structural relaxation times from TMDSC. At the highest temperature limit structural and secondary relaxation times obtained from ultrasound absorption are added. Solid and dashed lines are VFT and Arrhenius fits respectively. Crossover point on $\tau_\sigma(T)$ dependence determines T_g . Inset: Walden plot

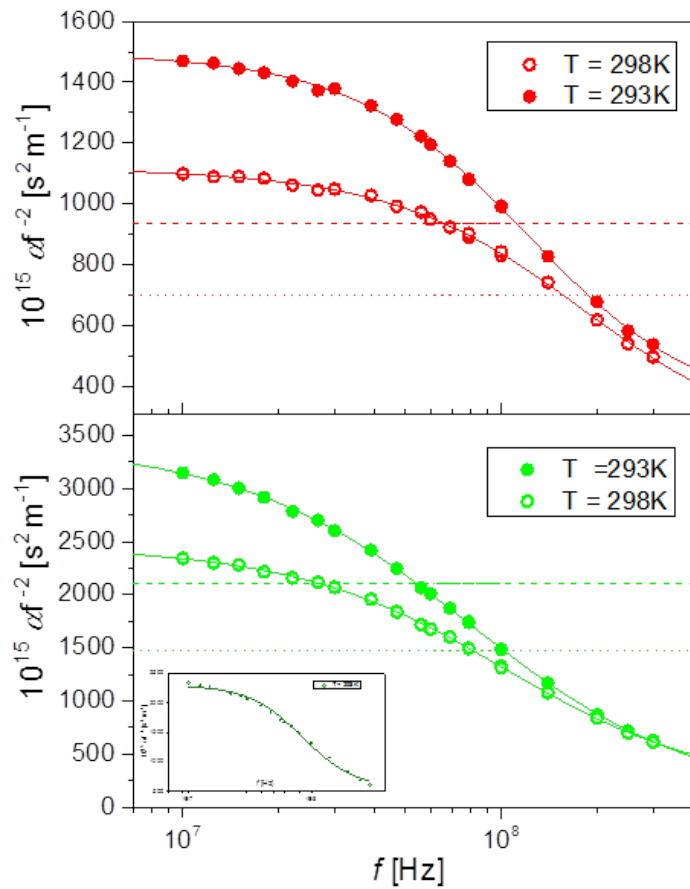


Figure 4

Ultrasound absorption coefficient per squared frequency $\cdot\alpha f^2$ versus $\log f$ for (upper panel) $(\text{EMIm})_2[\text{Co}(\text{NCS})_4]$ and (lower panel) $(\text{BMIm})_2[\text{Co}(\text{NCS})_4]$ at temperatures: 293.15 K (\bullet); and 298.15 K (\circ). Solid lines are fits by means of CC function. Dashed and dotted lines – classical absorption at temperatures 293.15 K and 298.15 K , respectively. The inset presents the fit with use of a single Debye function to ultrasonic spectrum for $(\text{BMIm})_2[\text{Co}(\text{NCS})_4]$ at 298.15 K .

References:

¹ Rooney, D.; Jacquemin, J.; Gardas, R. Thermophysical Properties of Ionic Liquids. *Top Curr. Chem.* **2009**, *290*, 185-212.

² Wellens, S.; Thijs, B.; Binnemans, K. How safe are protic ionic liquids? Explosion of pyrrolidinium nitrate. *Green Chem.* **2013**, *15*, 3484-3485.

³ Wojnarowska, Z.; Grzybowska, K.; Hawelek, L.; Swiety-Pospiech, A.; Masiewicz, E.; Paluch, M.; Sawicki, W.; Chmielewska, A.; Bujak, P.; Markowski, J. Molecular dynamics studies on the water mixtures of pharmaceutically important ionic liquid lidocaine HCl. *Mol. Pharm.* **2012**, *9*, 1250-1261.

⁴ Stoimenovski, J.; Dean, P. M.; Izgorodina, E. I.; MacFarlane, D. Protic pharmaceutical ionic liquids and solids: Aspects of protonics. *Faraday Discuss.*, **2012**, *154*, 335-352.

⁵ Yoshida, Y.; Saito, G. Influence of structural variations in 1-alkyl-3-methylimidazolium cation and tetrahalogenoferrate (III) anion on the physical properties of the paramagnetic ionic liquids. *J. Mater. Chem.* **2006**, *16*, 1254-1262.

⁶ Nockemann, P.; Thijs, B.; Postelmans, N.; Van Hecke, K.; Van Meervelt, L.; Binnemans, K. Anionic Rare-Earth Thiocyanate Complexes as Building Blocks for Low-Melting Metal-Containing Ionic Liquids, *J. Am. Chem. Soc.* **2006**, *128*, 13658-13659.

⁷ Peppel, T.; Kockerling, M.; Geppert-Rybczyńska, M.; Ralys, R. V.; Lehmann, J. K.; Verevkin, S. P.; Heintz, A. Low-Viscosity Paramagnetic Ionic Liquids with Doubly Charged $[\text{Co}(\text{NCS})_4]^{2-}$ Ions. *Angew. Chem. Int. Ed.* **2010**, *49*, 7116-7119.

⁸ Geppert-Rybczyńska, M.; Lehmann, J. K.; Peppel, T.; Kockerling, M.; Heintz, A. Studies of Physicochemical and Thermodynamic Properties of the Paramagnetic 1-Alkyl-3-methyl- imidazolium Ionic Liquids $(\text{EMIm})_2[\text{Co}(\text{NCS})_4]$ and $(\text{BMIm})_2[\text{Co}(\text{NCS})_4]$. *J. Chem. Eng. Data* **2010**, *55*, 5534-5538.

⁹ Novikov, V. N.; Sokolov, A. P. Universality of the dynamic crossover in glass-forming liquids: A “magic” relaxation time. *Phys. Rev. E* **2003**, *67*, 031507.

¹⁰ Casalini, R.; Roland, C. M. Scaling of the supercooled dynamics and its relation to the pressure dependences of the dynamic crossover and the fragility of glass formers. *Phys. Rev. B* **2005**, *71*, 014210.

¹¹ Ngai, K. L. *Relaxation and Diffusion in Complex Systems*; Springer Science + Business Media, New York 2011

¹² Hansen, C.; Stickel, F.; Berger, T.; Richert, R.; Fischer, E. W. Dynamics of Glass-Forming Liquids. III. Comparing the Dielectric α - and β -Relaxation of 1-propanol and o-terphenyl. *J. Chem. Phys.* **1997**, *107*, 1086-1093.

¹³ Sekula, M.; Pawlus, S.; Hensel-Bielowka, S.; Ziolo, J.; Paluch, M.; Roland, C. M. Structural and Secondary Relaxations in Supercooled Di-n-butyl Phthalate and Diisobutyl Phthalate at Elevated Pressure, *J. Phys. Chem. B* **2004**, *108*, 4997-5003.

¹⁴ Pawlus, S.; Kunal, K.; Hong, L.; Sokolov, A.P. Influence of molecular weight on dynamic crossover temperature in linear polymers. *Polymer* **2008**, *49*, 2918-2923

¹⁵ Stickel, F.; Fisher, E. W.; Richert R. Dynamics of Glass-Forming Liquids. I. Temperature-Derivative Analysis of Dielectric Relaxation Data. *J. Chem. Phys.* **1995**, *102*, 6251-6257.

¹⁶ Griffin, P.; Agapov, A.; Sokolov, A. Translation-rotation decoupling and nonexponentiality in room temperature ionic liquids. *Phys. Rev. E* **2012**, *86*, 021508.

¹⁷ Swiety-Pospiech, A.; Wojnarowska, Z.; Pionteck, J.; Pawlus, S.; Grzybowski, A.; Hensel-Bielowka, S.; Grzybowska, K.; Szulc, A.; Paluch, M. High pressure study of molecular dynamics of protic ionic liquid lidocaine hydrochloride. *J. Chem. Phys.* **2012**, *136*, 224501.

¹⁸ Pawlus, S.; Paluch, M.; Sekula, M.; Ngai, K. L.; Rzoska, S. J.; Ziolo, J. Changes in dynamic crossover with temperature and pressure in glass-forming diethyl phthalate. *Phys. Rev. E* **2003**, *68*, 021503

¹⁹ Behrends, R.; Kaatze, U. Hydrogen Bonding and Chain Conformational Isomerization of Alcohols Probed by Ultrasonic Absorption and Shear Impedance Spectrometry. *J. Phys. Chem. A* **2001**, *105*, 5829-5835.

²⁰ Wuensch, B. J.; Hueter, T. F.; Cohen, M. S. Ultrasonic Absorption in Castor Oil: Deviations from Classical Behavior. *J. Acoust. Soc. Am.* **1956**, 28, 311-312.

²¹ Zorębski, E.; Zorębski M. A Comparative Ultrasonic Relaxation Study of Lower Vicinal and Terminal Alkanediols at 298.15 K in Relation to Their Molecular Structure and Hydrogen Bonding. *J. Phys. Chem. B* **2014**, *118*, 5934-5942.

²² Zorębski, E.; Geppert-Rybczyńska, M.; Zorębski, M. Acoustics as a Tool for Better Characterization of Ionic Liquids: A Comparative Study of 1-Alkyl-3-methylimidazolium Bis[(trifluoromethyl)sulfonyl]imide Room-Temperature Ionic Liquids. *J. Phys. Chem. B* **2013**, *117*, 3867-3876.

²³ Makino, W.; Kishikawa, R.; Mozoshiri, M.; Takeda, S.; Yao, M. Viscoelastic Properties of Room Temperature Ionic Liquids. *J. Chem. Phys.* **2008**, *129*, 104510.

²⁴ Bhatia, A. B. *Ultrasonic absorption*; Clarendon Press, Oxford 1967.

²⁵ Jacobsen, B.; Niss, K.; Maggi, C.; Olsen, N.B.; Christensen, T.; Dyre, J.C; Beta relaxation in the shear mechanics of viscous liquids: Phenomenology and network modeling of the alpha-beta merging region. *J.Non-Cryst.Solids* **2011**, *357*, 267-273

²⁶ Kahle, S.; Schroter, K.; Hempel, E.; and Donth E. Calorimetric indications of a cooperativity onset in the crossover region of dynamic glass transition for benzoin isobutylether *J. Chem. Phys.* **1999**, *111*, 6462-6470 and the references within

²⁷ Fumino, K.; Wulf, A.; Ludwig, P. The potential role of hydrogen bonding in aprotic and protic ionic liquids. *Phys. Chem. Chem. Phys.* **2009**, *11*, 8790-8794.